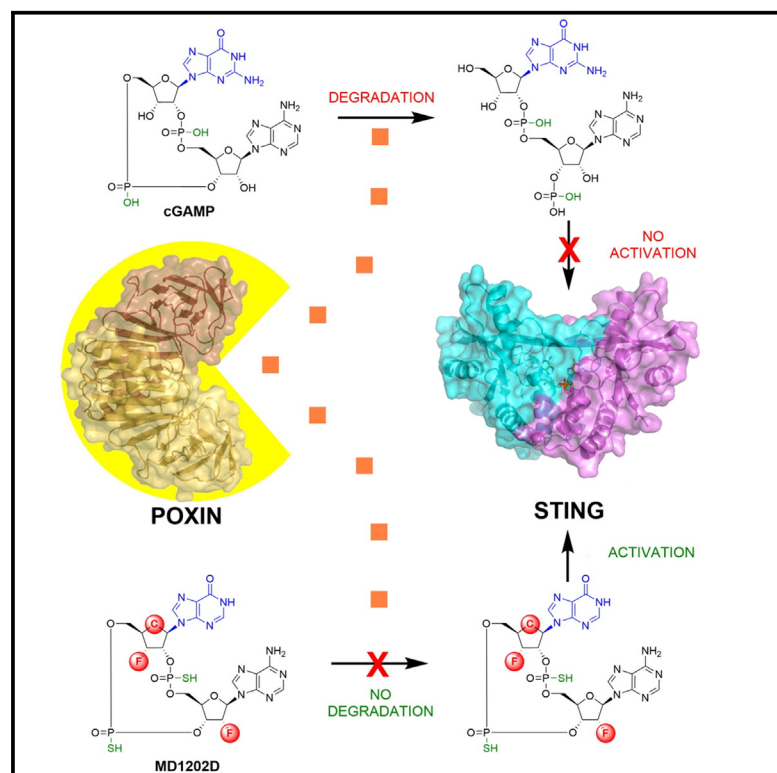# Fluorinated cGAMP analogs, which act as STING agonists and are not cleavable by poxins: Structural basis of their function

Graphical abstract

Authors

Martin Klima, Milan Dejmek,
Vojtech Duchoslav, ..., Gabriel Birkuš,
Radim Nencka, Evzen Boura

Correspondence

nencka@uochb.cas.cz (R.N.),
boura@uochb.cas.cz (E.B.)

In brief

Klima, Dejmek, Duchoslav et al. discover
MD1203 and MD1202D, which are
fluorinated cGAMP analogs targeting the
STING pathway with enhanced potency
and exhibit improved stability against
viral nucleases.

Highlights

- MD1203 and MD1202D described as high-affinity STING agonists

- MDs resist cleavage by viral nuclease poxin

- MDs' poxin binding differs from cGAMP yet is similar to cGAMP:STING binding mode

- MDs exhibit potential for antiviral development by offering enhanced stability

Article

Fluorinated cGAMP analogs, which act as STING agonists and are not cleavable by poxins: Structural basis of their function

Martin Klima,[1,2] Milan Dejmek,[1,2] Vojtech Duchoslav,[1,2] Andrea Eisenreichova,[1] Michal Sala,[1] Karel Chalupsky,[1] Dominika Chalupska,[1] Barbora Novotná,[1] Gabriel Birkuš,[1] Radim Nencka,[1,*] and Evzen Boura[1,3,*]

[1]Institute of Organic Chemistry and Biochemistry AS CR, v.v.i., Flemingovo nam. 2., 166 10 Prague 6, Czech Republic
[2]These authors contributed equally
[3]Lead contact
*Correspondence: nencka@uochb.cas.cz (R.N.), boura@uochb.cas.cz (E.B.)
https://doi.org/10.1016/j.str.2024.01.008

SUMMARY

The cGAS-STING pathway is a crucial part of innate immunity; it serves to detect DNA in the cytoplasm and to defend against certain cancers, viruses, and bacteria. We designed and synthesized fluorinated carbocyclic cGAMP analogs, MD1203 and MD1202D (MDs), to enhance their stability and their affinity for STING. These compounds demonstrated exceptional activity against STING. Despite their distinct chemical modifications relative to the canonical cyclic dinucleotides (CDNs), crystallographic analysis revealed a binding mode with STING that was consistent with the canonical CDNs. Importantly, MDs were resistant to cleavage by viral poxin nucleases and MDs-bound poxin adopted an unliganded-like conformation. Moreover, MDs complexed with poxin showed a conformation distinct from cGAMP bound to poxin, closely resembling their conformation when bound to STING. In conclusion, the development of MD1203 and MD1202D showcases their potential as potent STING activators with remarkable stability against poxin-mediated degradation—a crucial characteristic for future development of antivirals.

INTRODUCTION

Viruses pose a formidable threat to organisms across the evolutionary spectrum, including humans. They have evolved intricate strategies to infiltrate cells in order to replicate. Consequently, cells must possess a robust defense arsenal. One pivotal defense mechanism is the production of type I interferons (IFN I), which plays a fundamental role in establishing an antiviral response, including alerting neighboring cells to the presence of viral infection.[1,2]

Central to the induction of interferon production lies the cGAS-STING pathway, an essential molecular cascade in which cGAS (cyclic GMP-AMP synthase) serves as an innate immune sensor, adept at recognizing cytosolic dsDNA.[3,4] This includes pathogen-derived DNA arising from bacteria, DNA viruses, or reverse transcription of retroviruses, as well as self-DNA emanating from damaged or deceased cell nuclei or mitochondria.[5] Upon detection of cytosolic DNA, cGAS undergoes dimerization and generates 2′,3′-cyclic-GMP-AMP (cGAMP), which is a second messenger.[6,7] Once cGAMP binds to STING (stimulator of interferon genes), it initiates the entire signaling cascade. STING translocates from the endoplasmic reticulum to the Golgi, where it recruits and activates the TBK1 kinase. Consequently, TBK1 phosphorylates IRF3, culminating in its dimerization and nuclear translocation.[8] Once within the nucleus, IRF3 binds to specific DNA sequences, thereby initiating the transcriptional activation of type I interferon genes.[9]

However, viruses, in the course of their evolutionary trajectory, have developed strategies to overcome and undermine these intrinsic immune defenses of their host organisms.[4]

Poxins, a family of unusual nucleases specific to cGAMP, have recently been discovered in pox viruses (hence the name).[10] These enzymes enable the viruses to evade the host's innate immune system by degrading cGAMP, leading to the inhibition of the cGAS-STING pathway.[11] Crystal structures of vaccinia virus poxin in pre- and post-reactive states define the mechanism of selective cGAMP degradation through metal-independent cleavage of the 3′–5′ bond, converting cGAMP into linear Gp[2′–5′]Ap[3′].[10] Thus, poxins are used by viruses as an evasion mechanism that allows them to dampen the immune response mediated by cGAMP and potentially establish successful infection.

We have prepared a novel class of fluorinated cyclic dinucleotides that exhibit high potency against STING and are not cleavable by poxin. We have solved crystal structures of these compounds in complex with both STING and monkeypox virus (MpxV) poxin that explain their potency and stability.

RESULTS

Fluorinated cGAMP analogs

We decided to prepare carbocyclic cGAMP analogs fluorinated at the (pseudo)sugar rings because both of these modifications could lead to the increase in stability of the molecules[12] as well as in the
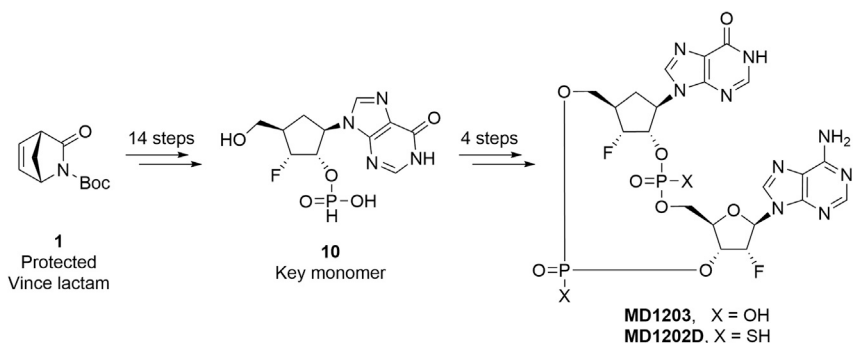
Figure 1. Simplified scheme of synthesis of MD1203 and MD1202D
The overall synthesis used a protected Vince lactam as starting material to synthesize a monomer that was subsequently chemically cyclized. Details are in Schemes S1 and S2.

affinity toward STING.[13] Through a straightforward, yet rather challenging syntheses (Scheme S1) starting from a protected Vince Lactam **1** we prepared the key intermediate **10** (Figure 1). This monomer was coupled and subsequently cyclized with 2′-fluoro-2′-deoxyadenosine phosphoramidite. The standard means of connecting both (thio)phosphate bonds were employed. The linear dinucleotide was formed using py-TFA/tBHP and py-TFA/xanthane hydride systems, respectively. Subsequently, the macrocycle was closed with DMOCP/iodine and DMOCP/beaucage reagent sequence, respectively (Figure 1 and Scheme S2). This resulted in the cyclic dinucleotides MD1203 and MD1202D (further referred to also as MDs) after deprotection using methylamine.

STING activity assay

The activities of the cyclic dinucleotides (CDNs) were assessed using our in-house prepared reporter HEK 293T ISRE cell lines.[14] Each of these cell lines expresses one of the five most common STING haplotypes found in the human population: R232 (WT), R71H-G230A-R293Q (HAQ), R232H (REF), G230A-R293Q (AQ), and R293Q (Q). These reporter cell lines have luciferase as a reporter, and luciferase expression is dependent on IRF3 (interferon regulatory factor 3) upon the interaction of STING with the CDNs. It's worth noting that these allelic forms of STING exhibit differences in their CDN binding capacities.[14,15]

The agonistic activity toward wild-type STING and its most abundant allelic forms (HAQ, REF, AQ, and Q) was evaluated using a cell-based reporter assay, in which we included digitonin A, a mild detergent, for cell membrane permeabilization[14,16,17] (Figure 2, Table S1, and Figure S1). Without this permeabilization, the negatively charged CDNs enter the cells only slowly, which significantly decreases their effectiveness. Both MD1203 and MD1202D proved to be very strong activators of STING across the WT, HAQ, and AQ of allelic variants, with their EC_{50} values similar or better than canonical CDNs and the former clinical candidate ADU-S100 (Figure 2, Table S1, and Figure S1). The important difference appeared in the case of REF and Q STING haplotypes that are present in about 13% and 1% of humans, respectively.[15,18] These two haplotypes have demonstrated lower binding efficiency to bacterial 3′,3′-CDNs and some synthetic 2′,3′-CDNs when compared to WT, HAQ, and Q haplotypes.[14,18]

Structural basis for the activation of STING by MD1203 and MD1202D

The atomic details of the interaction of STING with MDs were uncovered by the crystallographic analysis of the respective protein-ligand complexes. The obtained structures were in a good

agreement with previous crystallographic studies on the STING protein complexed with CDNs. MD1203 and MD1202D were bound to STING in a usual stoichiometry protein:CDN 2:1.[19] The dimer of the STING CDN-binding domain was present in the closed conformation with the lid formed above the ligand-binding site (Figure 3A). The binding of the adenine and guanine bases of MD1203 and MD1202D was mediated mainly by parallel π- π stacking with Tyr167 and by π-cation interactions and hydrogen bonds with Arg238. The macrocycles of MD1203 and MD1202D interacted with STING via hydrogen bonds and salt bridges with Ser162, Thr263, Thr267, and Arg238 (Figures 3B and 3C). Overall, the atomic details of the interactions of STING and MD1203, as well as MD1202D, exhibited similarities to the previously published structures of the STING-CDN complexes.[13,17,20,21]

Enzymatic stability of MD1203 and MD1202D

As mentioned previously, viruses use special nucleases, poxins, to degrade cGAMP. However, we speculated that the unique features of MDs, in which the (pseudo)sugar hydroxyl groups were replaced by fluorine atoms, will make these CDNs resistant to poxin-mediated hydrolysis while retaining the STING agonistic activity. The highly electronegative fluorine atom serves as a bio-isosteric substitute for the hydroxyl group, closely mimicking the naturally occurring CDNs.[13] We prepared a recombinant MpxV poxin and directly tested the stability of MDs in its presence. While 2′,3′-cGAMP was rapidly degraded by the poxin nuclease, both MD1203 and MD1202D exhibited remarkable stability, showing no degradation following a 12-h incubation at 37°C, a stability akin to that of 3′,3′-cGAMP (Figure 4).

MD1203 and MD1202D recognition by MpxV poxin

These compounds are not cleaved by poxins. However, we speculated that due to their chemical structure, which inherently resembles cGAMP, they would still bind and be recognized by poxins. Crystallography is increasingly used as an analytical tool by us and others.[22–26] We attempted to obtain crystals of MD1203 and MD1202D complexed with poxins to gain molecular insights into the poxins' recognition mechanism of these CDNs. Indeed, we successfully obtained well-diffracting crystals (1.65 Å and 1.93 Å, respectively, Table S2) for these complexes. The structures were determined using molecular replacement (detailed in the Materials and Methods section) and were refined to favorable R-factors and geometry (Table S2).

Poxins exist as dimers, and the binding site for CDNs is situated at the monomer-monomer interface.[10,11] As expected, both MDs were located at this interface and their density was clearly visible (Figure 5). Both MDs, like cGAMP, are non-symmetric; they have a hypoxanthine and an adenine base. The binding mode of the hypoxanthine base is the same in both
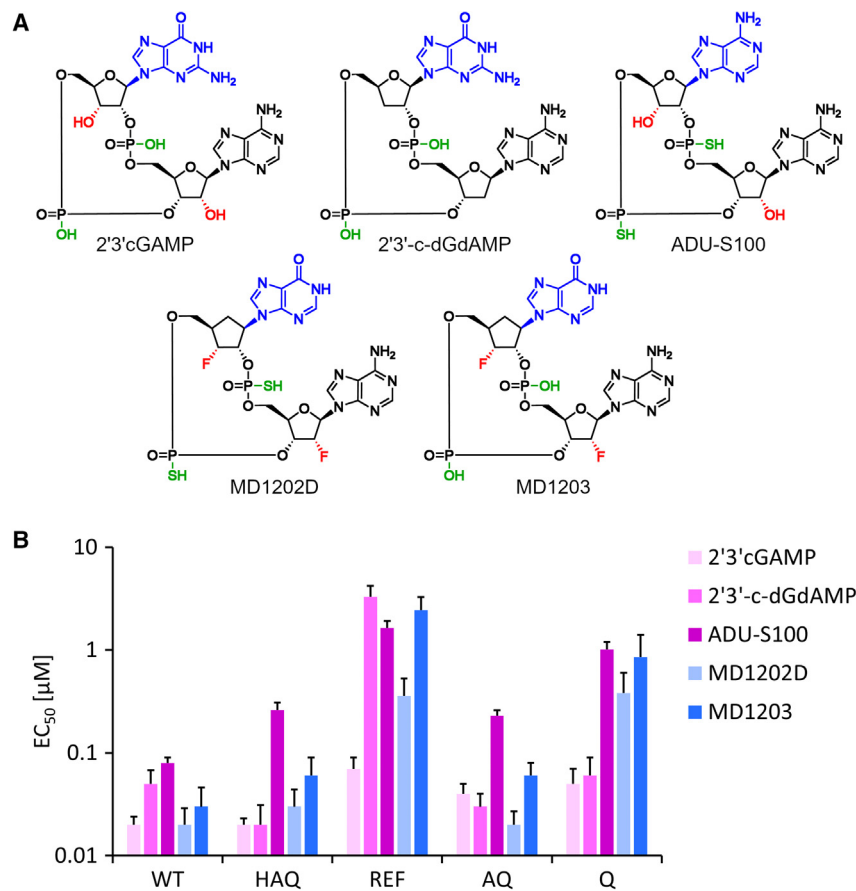
Figure 2. *In vitro* activity of selected CDNs in the digitonin HEK 293T cell-based reporter assay

(A) Schemes of CDNs used in the assay.

(B) EC_{50} values from the digitonin assay using 293T reporter cells expressing different STING protein haplotypes are expressed as mean ± SEM of at least two independent experiments measured in triplicates.

tion (Figures 6 and S2) and also the conformation of poxin bound MD compounds is different from that of poxin bound cGAMP (Figure 6C). Structurally, in case of the cGAMP, the guanine base forms a hydrogen bond with Ala18 through its amine group and with Lys186 through its oxygen atom, while Lys186 is not involved in the recognition of the hypoxanthine base in MDs. The adenine base forms a hydrogen bond with Asn149 in the case of cGAMP. However, in the case of MDs, yet again, this residue is not involved in the recognition of the adenine base. On the contrary, Tyr138, which is involved in the macrocycle binding in the case of cGAMP, is observed to participate in π-π stacking interactions with the adenine base of MDs. Moreover, Gly127, which is not involved in the binding of cGAMP, forms water bridges with MDs macrocycles. Chemically, the major differences between MDs and cGAMP are the exchange of the guanine base for the hypoxanthine base and fluorination of the ribose rings. It is unlikely that the hypoxanthine-guanine exchange is responsible for the different binding mode as the amine group of the adenine base does not form any bond with poxin.[10] The carba modification of one of the ribose rings is also unlikely to have caused this change, as this structural feature has never significantly affected behavior of CDNs toward STING.[13,14] However, fluorination of the (pseudo)ribose ring significantly improved binding of CDNs to STING by altering the enthalpy and entropy contributions. Interestingly, the crystal structures revealed the same binding conformation of STING,[13] which we also observed for MDs binding toward STING (Figure 7).

DISCUSSION

In this study, our aim was to prepare cGAMP analogs that would be resistant against the viral endonuclease poxin, which specifically cleaves cGAMP. So far only few analogs of cGAMP, phosphorothioate and dideoxy cGAMP, were described as poxin resistant.[10,27] The ribose 2′-hydroxyl group is essential for poxin mediated cleavage of cGAMP. It acts as a nucleophile induced by the amino group of poxin's Lys142 and attacks the bridging phosphate of the 3′–5′ phosphate. This subsequently leads to the cleavage of the bridge and, via 2′–3′ phosphate intermediate, ultimately leads to the linear dinucleotide.[10] However, simple dideoxy cGAMP analogs have certain disadvantages compared to the canonical 2′,3′-cGAMP as well as the difluorinated cGAMP analog. While

structures (Figures 5B and 5C), its oxygen atoms form a hydrogen bond with the sidechain of His17 and also bind the nitrogen atom of Ala18 (in the case of MD1203 through a water bridge or, in the case of MD1202D, directly), another water bridge is formed to Tyr138 of the other poxin monomer. This monomer also forms several water bridges, mainly through Arg182, Arg184, Gln169, and Gly127, to the macrocycles of MD1202D and MD1203. However, the adenine base adapts a different orientation in each structure. It undergoes an approximate 180-degree rotation relative to the adenine of the other CDN. Intriguingly, both conformations facilitate π-π stacking with the aromatic ring of Tyr138. But only the conformation observed in the case of MD1202D also allows for a hydrogen bond to His17 (Figure 5C). Nevertheless, both conformations are allowed and, most likely, exist in a dynamic equilibrium. This is supported by the fact that the B-factors for the adenine base are notably high (55–60), implying considerable mobility. In contrast, the B-factors for the hypoxanthine base are comparatively low (30–40), suggesting that this base is well fixed in its position (Figures 5D and 5E).

We expected that MDs-bound poxin would adopt the same conformation as cGAMP-bound poxin. Interestingly, this was not the case. cGAMP binding induces a movement of the α1 helix (by approximately 3 Å), causing a narrowing of the CDN binding site (Figure S2). However, upon structural comparison of MDs-bound or cGAMP-bound poxin with the unliganded poxin, we found that MDs-bound poxin adopts an unliganded-like conforma-
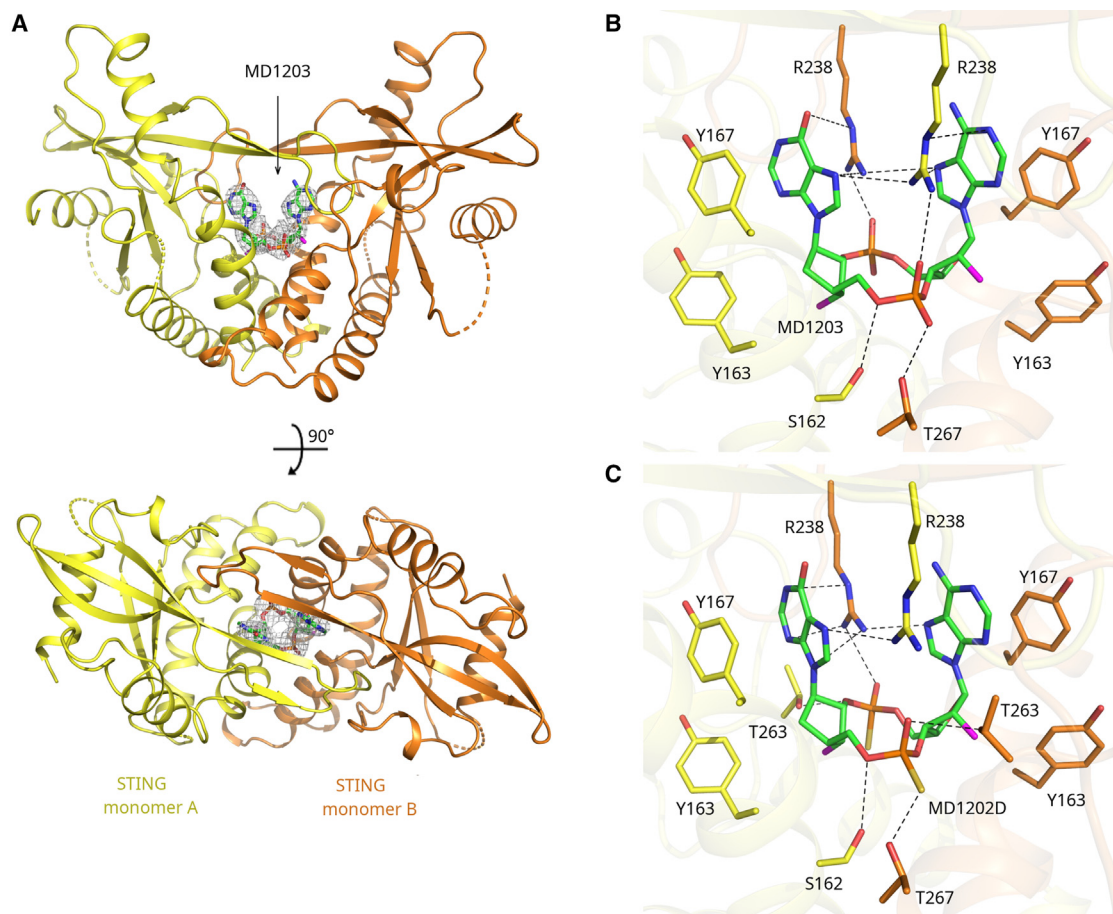
Figure 3. Crystal structure of human STING in complex with MD1203 and MD1202D

(A) Overall view of the STING/MD1203 complex. The protein backbone is shown in cartoon representation; the two STING monomers are depicted in yellow and orange. MD1203 is shown in stick representation and colored according to elements: carbon, green; nitrogen, blue; oxygen, red; phosphorus, orange; fluorine; magenta. The *Fo-Fc* omit map contoured at 3σ is shown around the ligand.

(B and C) Detailed view of the ligand binding site. MD1203 (B) or MD1202D (C) and side chains of selected STING residues are shown in stick representation with carbon atoms colored according to the protein/ligand assignment and other elements colored as in a. Selected hydrogen bonds involved in the STING-ligand interaction are presented as dashed black lines.

the dideoxy analogs perform exceptionally well in assays using digitonin-permeabilized cells, they show reduced activity on the REF allelic form of STING and display notably decreased performance in standard, unpermeabilized cells, possibly due to their impaired cellular uptake.[13,14] We hypothesized that by using carba-CDNs with the hydroxyl groups substituted by fluorine atoms, we could create an exceptionally active STING agonist.

These agonists would effectively target all STING isoforms, resist poxin-induced cleavage, and exhibit stability against nucleoside hydrolases. We prepared two such compounds: a CDN phosphate, MD1203, and a phosphorothioate, MD1202D. Both of these compounds indeed demonstrated outstanding biological activities against the wild-type STING and its HAQ, AQ, and Q allelic forms. Additionally, thiophosphate MD1202D outperformed
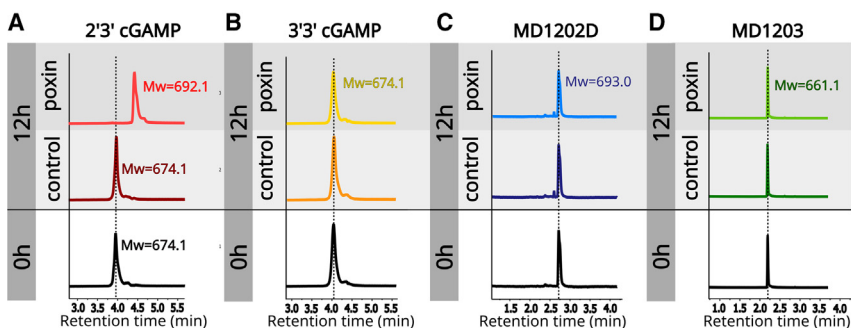

Figure 4. Stability of selected CDNs against poxin cleavage

Absorbance data (254 nm) obtained during UPLC-MS analysis of poxin reaction mixtures with (A) 2′,3′-cGAMP, (B) 3′,3′-cGAMP, (C) MD1202D, and (D) MD1203 are shown. Each compound underwent a 12-h incubation at 37°C with or without poxin, followed by analysis. Degradation of 2′,3′-cGAMP leads to a compound with Mw of 692.1 while the other CDNs remain stable.
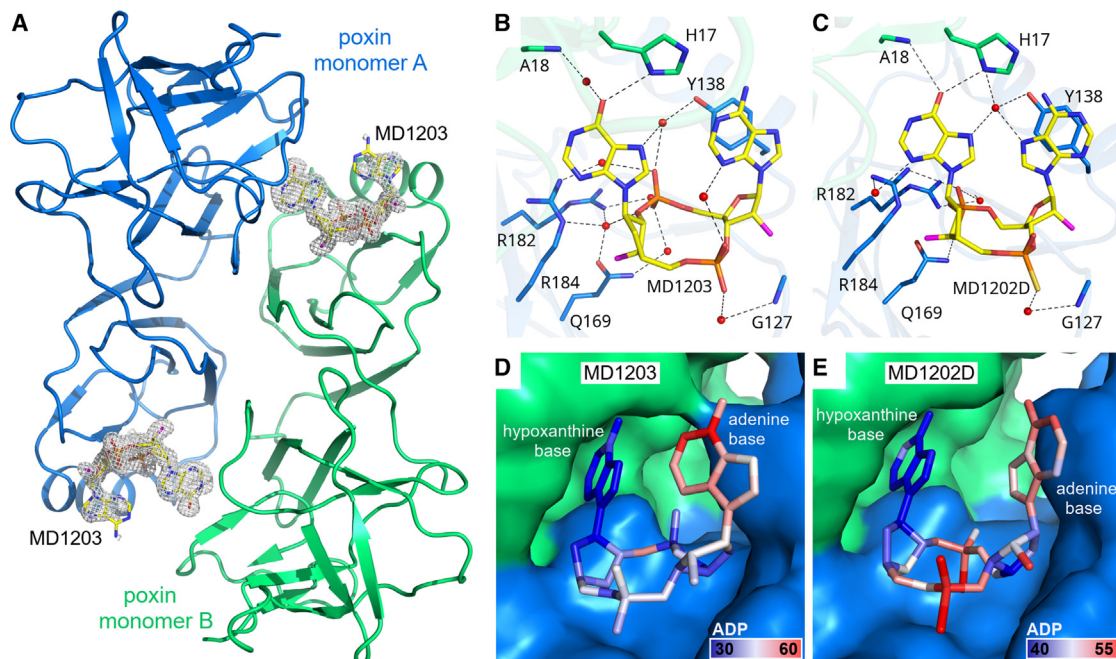
Figure 5. Crystal structure of MpxV poxin in complex with MD1203

(A) Overall view of the poxin/MD1203 complex depicted as in Figure 3A. The two poxin monomers are colored in blue and green, MD1203 carbons in yellow. The *Fo-Fc* omit map contoured at 3σ is shown around the two ligands.

(B and C) Detailed view of the MD1203 (B) and MD1202D (C) ligand binding site depicted as in Figure 3B.

(D and E) MD1203 (D) or MD1202D (E) are colored according to the atomic displacement parameters (ADPs, also known as *B* factors) using the gradient from blue (atoms with lowest ADPs) to red (atoms with highest ADPs). The protein molecules are shown in surface representation.

the ex-clinical trials candidate ADU-S100 and dideoxy-cGAMP by an order of magnitude against the REF allelic form (Figure 2, Table S1, and Figure S1). Intriguingly, the conformation of poxin when bound to MDs is almost identical to the conformation of un-liganded poxin (Figure S2), implying that cGAMP can induce conformational changes that the MD compounds cannot.

In conclusion, these non-hydrolyzable, stable cGAMP analogs possess significant potential in antiviral therapy. They effectively bypass viruses' defense mechanisms involving poxin nucleases that aim to prevent STING pathway activation. The compounds presented here demonstrate remarkable biological activity toward STING. However, further research is needed, including
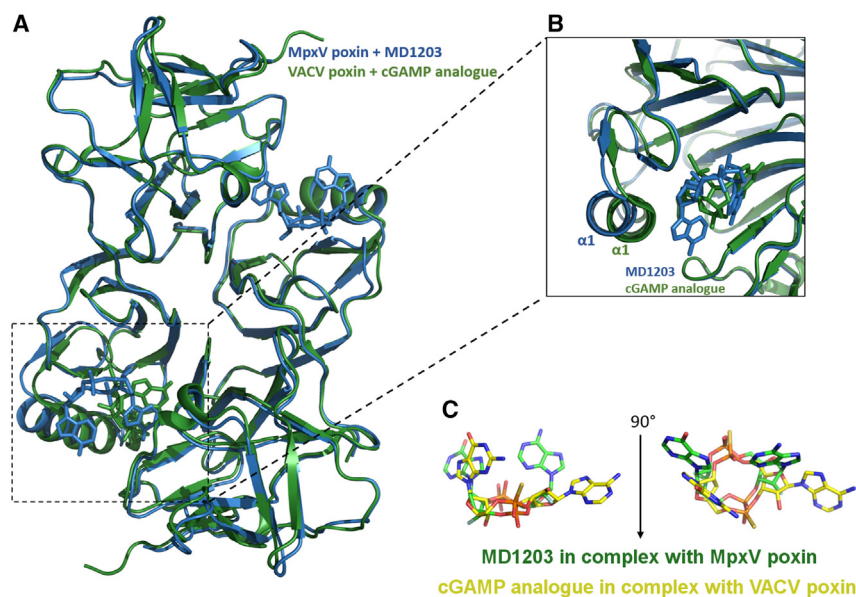

Figure 6. Conformational changes induced in VACV poxin by ligand binding

(A) Structural alignment of VACV poxin in complex with a non-hydrolyzable cGAMP analog, depicted in green (PDB code: 6EA8), and MpxV poxin in complex with MD1203, depicted in blue. cGAMP binding to the VACV poxin induces conformational changes of α-helix 1.

(B) Close-up on the conformational changes of α-helix 1.

(C) Superposition of cGAMP bound to VACV poxin and MD1203 bound to MpxV poxin. cGAMP is depicted in green and MD1203 in yellow.
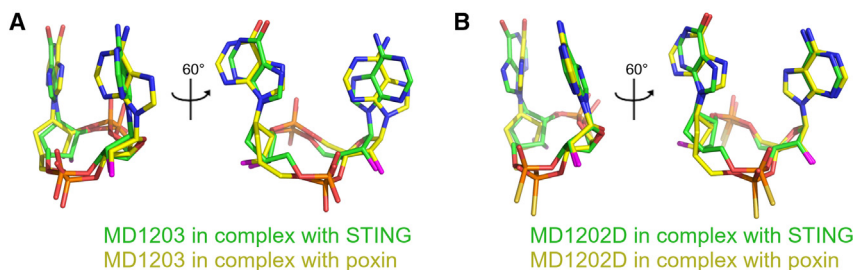
MD1203 in complex with MpxV poxin
cGAMP analogue in complex with VACV poxin

Figure 7. Conformations of MD1203 and MD1202D
(A) Superposition of MD1203 bound to poxin and STING. MD1203 is shown in stick representation with carbon atoms colored in yellow (in complex with poxin) or green (in complex with STING) and other elements colored as in Figure 3A. The protein molecules are not shown.
(B) Superposition of MD1202D bound to poxin and STING depicted as in a.

enhancement of cell-membrane permeation, which represents a challenge for all charged molecules. Alternatively, the design of compounds derived from CDNs that no longer bind to STING but display a high affinity for poxins is another approach. This strategy could selectively hinder viral activity while leaving the STING pathway unaffected in uninfected cells.

STAR★METHODS

Detailed methods are provided in the online version of this paper and include the following:

- KEY RESOURCES TABLE
- RESOURCE AVAILABILITY
  - Lead contact
  - Materials availability
  - Data and code availability
- EXPERIMENTAL MODEL AND STUDY PARTICIPANT DETAILS
  - Bacterial strains
  - Cell lines
- METHOD DETAILS
  - Synthesis
  - Protein expression and purification
  - Crystallization and crystallographic analysis
  - Differential scanning fluorimetry (DSF)
  - Digitonin 293T STING reporter assay
  - Standard 293T STING reporter assay
  - Poxin activity assay
- QUANTIFICATION AND STATISTICAL ANALYSIS
  - Activity of CDNs in cell-based reporter assays
  - Crystallographic data collection and processing

SUPPLEMENTAL INFORMATION

Supplemental information can be found online at https://doi.org/10.1016/j.str.2024.01.008.

REFERENCES

1. Murira, A., and Lamarre, A. (2016). Type-I Interferon Responses: From Friend to Foe in the Battle against Chronic Viral Infection. Front. Immunol. 7, 609.

2. Schoggins, J.W. (2019). Interferon-Stimulated Genes: What Do They All Do? Annu. Rev. Virol. 6, 567–584.

3. Ma, Z., and Damania, B. (2016). The cGAS-STING Defense Pathway and Its Counteraction by Viruses. Cell Host Microbe 19, 150–158.

4. Hopfner, K.P., and Hornung, V. (2020). Molecular mechanisms and cellular functions of cGAS-STING signalling. Nat. Rev. Mol. Cell Biol. 21, 501–521.

5. Motwani, M., Pesiridis, S., and Fitzgerald, K.A. (2019). DNA sensing by the cGAS-STING pathway in health and disease. Nat. Rev. Genet. 20, 657–674.

6. Kato, K., Omura, H., Ishitani, R., and Nureki, O. (2017). Cyclic GMP-AMP as an Endogenous Second Messenger in Innate Immune Signaling by Cytosolic DNA. Annu. Rev. Biochem. 86, 541–566.

7. Su, M., Zheng, J., Gan, L., Zhao, Y., Fu, Y., and Chen, Q. (2022). Second messenger 2'3'-cyclic GMP-AMP (2'3'-cGAMP): Synthesis, transmission, and degradation. Biochem. Pharmacol. 198, 114934.

8. Tanaka, Y., and Chen, Z.J. (2012). STING Specifies IRF3 Phosphorylation by TBK1 in the Cytosolic DNA Signaling Pathway. Sci. Signal. 5, ra20.

9. Negishi, H., Taniguchi, T., and Yanai, H. (2018). The Interferon (IFN) Class of Cytokines and the IFN Regulatory Factor (IRF) Transcription Factor Family. Csh Perspect Biol 10, a028423.

10. Eaglesham, J.B., Pan, Y., Kupper, T.S., and Kranzusch, P.J. (2019). Viral and metazoan poxins are cGAMP-specific nucleases that restrict cGAS-STING signalling. Nature 566, 259–263.

11. Eaglesham, J.B., McCarty, K.L., and Kranzusch, P.J. (2020). Structures of diverse poxin cGAMP nucleases reveal a widespread role for cGAS-STING evasion in host-pathogen conflict. Elife 9, e59753.

12. Marquez, V.E. (1996). Carbocyclic nucleosides. Adv. Antivir. Drug Des. 2, 89–146.

13. Smola, M., Gutten, O., Dejmek, M., Kožíšek, M., Evangelidis, T., Tehrani, Z.A., Novotná, B., Nencka, R., Birkuš, G., Rulíšek, L., and Boura, E. (2021). Ligand Strain and Its Conformational Complexity Is a Major

Factor in the Binding of Cyclic Dinucleotides to STING Protein. Angew. Chem., Int. Ed. Engl. 60, 10172–10178.

14. Novotná, B., Vaneková, L., Zavřel, M., Buděšínský, M., Dejmek, M., Smola, M., Gutten, O., Tehrani, Z.A., Pimková Polidarová, M., Brázdová, A., et al. (2019). Enzymatic Preparation of 2'-5',3'-5'-Cyclic Dinucleotides, Their Binding Properties to Stimulator of Interferon Genes Adaptor Protein, and Structure/Activity Correlations. J. Med. Chem. 62, 10676–10690.

15. Patel, S., and Jin, L. (2019). TMEM173 variants and potential importance to human biology and disease. Gene Immun. 20, 82–89.

16. Dejmek, M., Brazdova, A., Otava, T., Polidarova, M.P., Klíma, M., Smola, M., Vavrina, Z., Buděšínský, M., Dračínský, M., Liboska, R., et al. (2023). Vinylphosphonate-based cyclic dinucleotides enhance STING-mediated cancer immunotherapy. Eur. J. Med. Chem. 259, 115685.

17. Pimková Polidarová, M., Břehová, P., Kaiser, M.M., Smola, M., Dračínský, M., Smith, J., Marek, A., Dejmek, M., Šála, M., Gutten, O., et al. (2021). Synthesis and Biological Evaluation of Phosphoester and Phosphorothioate Prodrugs of STING Agonist 3',3'-c-Di(2'F,2'dAMP). J. Med. Chem. 64, 7596–7616.

18. Yi, G., Brendel, V.P., Shu, C., Li, P., Palanathan, S., and Cheng Kao, C. (2013). Single nucleotide polymorphisms of human STING can affect innate immune response to cyclic dinucleotides. PLoS One 8, e77846.

19. Huang, Y.H., Liu, X.Y., Du, X.X., Jiang, Z.F., and Su, X.D. (2012). The structural basis for the sensing and binding of cyclic di-GMP by STING. Nat. Struct. Mol. Biol. 19, 728–730.

20. Dejmek, M., Šála, M., Brazdova, A., Vanekova, L., Smola, M., Klíma, M., Břehová, P., Buděšínský, M., Dračínský, M., Procházková, E., et al. (2022). Discovery of isonucleotidic CDNs as potent STING agonists with immunomodulatory potential. Structure 30, 1146–1156.e11.

21. Vavřina, Z., Perlíková, P., Milisavljević, N., Chevrier, F., Smola, M., Smith, J., Dejmek, M., Havlíček, V., Buděšínský, M., Liboska, R., et al. (2022). Design, Synthesis, and Biochemical and Biological Evaluation of Novel 7-Deazapurine Cyclic Dinucleotide Analogues as STING Receptor Agonists. J. Med. Chem. 65, 14082–14103.

22. Silhan, J., Klima, M., Otava, T., Skvara, P., Chalupska, D., Chalupsky, K., Kozic, J., Nencka, R., and Boura, E. (2023). Discovery and structural characterization of monkeypox virus methyltransferase VP39 inhibitors reveal similarities to SARS-CoV-2 nsp14 methyltransferase. Nat. Commun. 14, 2259.

23. Mejdrová, I., Chalupská, D., Plačková, P., Müller, C., Šála, M., Klíma, M., Baumlová, A., Hřebabecký, H., Procházková, E., Dejmek, M., et al. (2017). Rational Design of Novel Highly Potent and Selective Phosphatidylinositol 4-Kinase IIIbeta (PI4KB) Inhibitors as Broad-Spectrum Antiviral Agents and Tools for Chemical Biology. J. Med. Chem. 60, 100–118.

24. Maveyraud, L., and Mourey, L. (2020). Protein X-ray Crystallography and Drug Discovery. Molecules 25.

25. Kroeck, K.G., Sacco, M.D., Smith, E.W., Zhang, X., Shoun, D., Akhtar, A., Darch, S.E., Cohen, F., Andrews, L.D., Knox, J.E., and Chen, Y. (2019).

26. Skvara, P., Chalupska, D., Klima, M., Kozic, J., Silhan, J., and Boura, E. (2023). Structural basis for RNA-cap recognition and methylation by the mpox methyltransferase VP39. Antivir. Res. 216, 105663.

27. Stazzoni, S., Böhmer, D.F.R., Hernichel, F., Özdemir, D., Pappa, A., Drexler, D., Bauernfried, S., Witte, G., Wagner, M., Veth, S., et al. (2022). Novel Poxin Stable cGAMP-Derivatives Are Remarkable STING Agonists. Angew. Chem., Int. Ed. Engl. 61, e202207175.

28. Duchoslav, V., and Boura, E. (2023). Structure of monkeypox virus poxin: implications for drug design. Arch. Virol. 168, 192.

29. Smola, M., Birkus, G., and Boura, E. (2019). No magnesium is needed for binding of the stimulator of interferon genes to cyclic dinucleotides. Acta Crystallogr. F Struct. Biol. Commun. 75, 593–598.

30. Mueller, U., Förster, R., Hellmig, M., Huschmann, F.U., Kastner, A., Malecki, P., Pühringer, S., Röwer, M., Sparta, K., Steffien, M., et al. (2015). The macromolecular crystallography beamlines at BESSY II of the Helmholtz-Zentrum Berlin: Current status and perspectives. Eur. Phys. J. A 130, 141.

31. Kabsch, W. (2010). Xds. Acta Crystallogr. D Biol. Crystallogr. 66, 125–132.

32. Sparta, K.M., Krug, M., Heinemann, U., Mueller, U., and Weiss, M.S. (2016). Xdsapp2.0. J. Appl. Crystallogr. 49, 1085–1092.

33. Zhang, X., Shi, H., Wu, J., Zhang, X., Sun, L., Chen, C., and Chen, Z.J. (2013). Cyclic GMP-AMP Containing Mixed Phosphodiester Linkages Is An Endogenous High-Affinity Ligand for STING. Mol. Cell 51, 226–235.

34. McCoy, A.J., Grosse-Kunstleve, R.W., Adams, P.D., Winn, M.D., Storoni, L.C., and Read, R.J. (2007). Phaser crystallographic software. J. Appl. Crystallogr. 40, 658–674.

35. Afonine, P.V., Grosse-Kunstleve, R.W., Echols, N., Headd, J.J., Moriarty, N.W., Mustyakimov, M., Terwilliger, T.C., Urzhumtsev, A., Zwart, P.H., and Adams, P.D. (2012). Towards automated crystallographic structure refinement with phenix.refine. Acta Crystallogr. D Biol. Crystallogr. 68, 352–367.

36. Liebschner, D., Afonine, P.V., Baker, M.L., Bunkóczi, G., Chen, V.B., Croll, T.I., Hintze, B., Hung, L.W., Jain, S., McCoy, A.J., et al. (2019). Macromolecular structure determination using X-rays, neutrons and electrons: recent developments in Phenix. Acta Crystallogr. D 75, 861–877.

37. Emsley, P., Lohkamp, B., Scott, W.G., and Cowtan, K. (2010). Features and development of Coot. Acta Crystallogr. D Biol. Crystallogr. 66, 486–501.

38. Vavřina, Z., Gutten, O., Smola, M., Zavřel, M., Aliakbar Tehrani, Z., Charvát, V., Kožíšek, M., Boura, E., Birkuš, G., and Rulíšek, L. (2021). Protein-Ligand Interactions in the STING Binding Site Probed by Rationally Designed Single-Point Mutations: Experiment and Theory. Biochemistry 60, 607–620.

STAR★METHODS

KEY RESOURCES TABLE

REAGENT or RESOURCE	SOURCE	IDENTIFIER
Bacterial and virus strains		
Escherichia coli BL21 DE3 NiCo strain	New England Biolabs	Cat# C2529H
Chemicals, peptides, and recombinant proteins		
2′3′cGAMP	InvivoGen	Cat# tlrl-nacga23-1
ADU-S100	InvivoGen	Cat# tlrl-nacda2r
HisPur Ni-NTA Superflow Agarose	Thermo Fisher Scientific	Cat# 25216
Critical commercial assays		
Bright-Glo Luciferase Assay System	Promega	Cat# E2610
Deposited data		
poxin + MD1203	this publication	PDB: 8ORV
poxin + MD1202D	this publication	PDB: 8P44
STING + MD1203	this publication	PDB: 8ORW
STING + MD1202D	this publication	PDB: 8P45
Experimental models: Cell lines		
HEK 293T ISRE wt STING	Novotna et al.,[14]	N/A
HEK 293T ISRE R293Q STING	Novotna et al.,[14]	N/A
HEK 293T ISRE R232H STING	Novotna et al.,[14]	N/A
HEK 293T ISRE G230A-R293Q STING	Novotna et al.,[14]	N/A
HEK 293T ISRE R71H-G230A-R293Q STING	Novotna et al.,[14]	N/A
Recombinant DNA		
plasmid pSUMO-STING	Smola et al.,[13]	N/A
plasmid pSUMO-poxin	Duchoslav and Boura,[28]	N/A
Software and algorithms		
XDS	Kabsch et al.,[31]	https://xds.mr.mpg.de/
XDSapp v3.1.9	Sparta et al.,[32]	https://www.helmholtz-berlin.de/forschung/oe/em/soft-matter/forschung/bessy-mx/xdsapp/index_en.html
Phenix v1.20.1-4487	Liebschner et al.,[36]	https://phenix-online.org/
Coot v0.9.8.7	Emsley et al.,[37]	https://www2.mrc-lmb.cam.ac.uk/personal/pemsley/coot/
Grade2 v1.3.1	Global Phasing Ltd.	https://grade.globalphasing.org/cgi-bin/grade2_server.cgi
PyMol v2.5.4	Schrödinger, LLC	https://pymol.org/
Prism 7.05	GraphPad Software	https://www.graphpad.com/

RESOURCE AVAILABILITY

Lead contact
Further information and requests for resources and reagents should be directed to and will be fulfilled by the lead contact, Evzen Boura (boura@uochb.cas.cz).

Materials availability
All unique/stable reagents generated in this study will be made available on request, but we may require a payment and/or a completed materials transfer agreement if there is potential for commercial application.

Data and code availability

- The structural data (atomic coordinates and structural factors) have been deposited in the Protein Data Bank (https://www.rcsb.org) and are publicly available as of the date of publication. Accession numbers are listed in the key resources table.
- This paper does not report original code.
- Any additional information required to reanalyze the data reported in this paper is available from the lead contact upon request.

EXPERIMENTAL MODEL AND STUDY PARTICIPANT DETAILS

Bacterial strains

All proteins used for biochemical studies were recombinantly expressed in Escherichia coli BL21 DE3 NiCo strain (New England Biolabs, C2529H).

Cell lines

All cell-based assay studies were performed using stably transfected cell lines derived from commercially available HEK 293T cells (ATCC, CRL-3216). They are human epithelial-like cells originally isolated from a single healthy, electively terminated female fetus of unknown parentage. The cells were cultivated in DMEM medium with high glucose supplemented with 10% heat inactivated FBS at 37°C with 5% CO2.

METHOD DETAILS

Synthesis

Conventional techniques of organic chemistry were employed and are described in detail, along with the NMR spectra, in the Supplementary Information. 2′3′cGAMP and ADU-S100 were purchased from InvivoGen and used as received. 2′3′-c-dGdAMP was synthesized according to a procedure published by us.[14] Briefly, nucleoside triphosphates (dATP and dGTP, final concentration 1 mM) were incubated in 20 mM Tris-HCl buffer, pH 8.0, containing 20 mM MgCl2, 5 μM mouse cGAS, and 0.1 mg/mL herring testes DNA at 37°C overnight in a shaker. The reaction mixtures were then spun at 25000g for 20 min, and supernatants were passed through Pierce Protein Concentrators PES, 3000 MWCO, 0.5 mL (Thermo Fisher Scientific, Prague, Czech Republic). Triethylammonium bicarbonate buffer (pH 8.5) was added to the flow-through fractions to 0.1 M final concentration, and CDNs were purified on a semipreparative C18 column (Luna 5 μm C18 250 mm × 10 mm) using 50 min gradient at flow rate 3 mL/min of 0−10% acetonitrile in 0.1 M TEAB buffer (pH 8.5). TEAB was removed from the collected fractions by 3 cycles of evaporation/dissolution in 50% methanol, and triethylammonium ion was exchanged for Na+ ion by slowly passing aqueous solution of the TEA+ salt through a DOWEX 50 (Na+ cycle) column and freeze-drying appropriate eluted fractions. For further details of the synthesis, please, see Methods S1. The NMR spectra of the products can be found in Data S1.

Protein expression and purification

Poxin (Uniprot accessions code Q5IXL2, amino acid residues 1-197) and STING (Uniprot accession code Q86WV6, amino acid residues 140-343) proteins were purified using the same protocols as before.[28,29] Briefly, they were expressed as fusion proteins with the 8xHis-SUMO tag, which facilitates purification and enhances solubility. The proteins were expressed in the *E. coli* BL21 DE3 Star and NiCo bacterial strains, respectively, in the autoinduction ZY-5052 medium. Bacterial cells expressing poxin or STING were harvested by centrifugation and disrupted by sonication or using the Emulsiflex C3 instrument (Avestin) in the lysis buffer (50 mM Tris pH 8.0, 300 mM NaCl, 20 mM imidazole, 10% glycerol, 3 mM β-mercaptoethanol), respectively. The lysates were precleared with centrifugation for 30 min at 30,000 g and incubated with the HisPur Ni-NTA Superflow agarose (Thermo Fisher Scientific) for 60 min. Then, the agarose beads were extensively washed with the lysis buffer (STING) or with the lysis buffer containing 1 M NaCl (poxin) and the proteins of interest were eluted with the elution buffer (50 mM Tris pH 8, 300 mM NaCl, 300 mM imidazole, 10% glycerol, 3 mM β-mercaptoethanol). The His$_8$-SUMO tag was cleaved overnight with the recombinant yeast Ulp1 protease. Poxin was dialyzed against the lysis buffer and the 8xHis-SUMO tag was removed by reverse Ni-NTA chromatography. The resulting protein was further purified using the size exclusion chromatography at the HiLoad 16/600 Superdex 75 prep grade column (Cytiva) in the SEC buffer (20 mM HEPES pH 7.5, 250 mM KCl, 0.5 mM TCEP). STING was purified using the size exclusion chromatography at the HiLoad 16/600 Superdex 75 prep grade column (Cytiva) in the buffer A (50 mM Tris pH 7.4, 50 mM NaCl) followed by the anion exchange chromatography at the HiTrap Q HP column (Cytiva) using a gradient from the buffer A to the buffer B (50 mM Tris pH 7.4, 1M NaCl). The purified proteins were concentrated to 15-20 mg/ml, aliquoted, flash frozen in liquid nitrogen, and stored at 193 K until required.

Crystallization and crystallographic analysis

Poxin was crystallized using similar protocols as before.[28] Briefly, the protein was supplemented with 2 mM MD1203 or MD1202D. The initial poorly diffracting crystals obtained in the JCSG screens (Qiagen) were used to prepare micro-seeds – the whole drops containing these crystals were resuspended in 100 μl of the seed buffer (100 mM HEPES pH 7.5, 20% w/v PEG 8000), intensively vortexed for 5 min, and diluted to 10^{-4} in the seed buffer. These seeds were immediately used for crystallization at the 1:5 (seed:protein) ratio using the Mosquito pipetting robot (SPT Labtech). STING was supplemented with 10 mM EDTA, which improves the quality

of STING crystals,[29] and 1 mM MD1203 or MD1202D. Diffraction quality crystals were obtained in sitting drops composed of 300 nl of protein with the indicated ligand and 300 nl of mother liquor (for poxin/MD1203: 100 mM phosphate-citrate pH 4.2, 40% PEG 300; for poxin/MD1202D: 200 mM NH$_4$NO$_3$, 20% PEG 3 350; for STING/MD1203: 100 mM Tris pH 8.0, 20% PEG 8.000, 200 mM LiCl; for STING/MD1202D: 100 mM HEPES pH 7.5, 20% PEG 4.000, 200 mM NaCl). The crystals grew within a range of 24 to 72 hours at room temperature. Upon harvest, the crystals were cryo-protected in the well solution supplemented with 20% glycerol (except for crystals of poxin/MD1203 that did not require cryo-protection) and flash cooled in liquid nitrogen. The datasets were collected from single crystals on the BL14.1 beamline at the BESSY II electron storage ring operated by the Helmholtz-Zentrum Berlin.[30]

The data were integrated and scaled using XDSapp v3.1.9.[31,32] Structures of the MpxV poxin and human STING proteins in complexes with MD1203 or MD1202D were solved by molecular replacement using the structures of vaccinia virus poxin (pdb entry 6EA6[10]) and the STING/cGAMP complex (pdb entry 4KSY[33]) as search models, respectively. Initial models were obtained with Phaser v2.8.3.[34] The models were further improved using automatic model refinement with the phenix.refine tool[35] from the Phenix package v1.20.1-4487[36] and manual model building with Coot v0.9.8.7.[37] Geometrical restraints for the ligands were generated with Grade2 v1.3.1 (Global Phasing Ltd.). Statistics for data collection and processing, structure solution and refinement were calculated with the phenix.table_one tool and are summarized in Table S2. Structural figures were generated with the PyMOL Molecular Graphics System v2.5.4 (Schrödinger, LLC). The atomic coordinates and structural factors were deposited in the Protein Data Bank (https://www.rcsb.org).

Differential scanning fluorimetry (DSF)
The stability of protein-ligand complex was examined by the DSF method as previously described.[20,38] **Briefly, the DSF was run** in **96-well optical plates** (LightCycler® 480 Multiwell Plate 96 white, Roche). STING protein WT and AQ allelic forms were used. Thermal denaturation of samples was performed on a LightCycler 480 Instrument II (Roche). The first derivative of fluorescence intensity referring to thermal denaturation of the protein was determined as melting temperatures (T_m), and the thermal shift (ΔT_m) was calculated as the difference of T_m of ligand-free and protein in complex with CDN.

Digitonin 293T STING reporter assay
The activity of tested CDNs was determined using reporter HEK 293T ISRE cell lines expressing various STING protein haplotypes in digitonin (R232 (WT), R293Q (Q), R232H (REF), G230A-R293Q (AQ), R71H-G230A-R293Q (HAQ) allelic forms) and standard (WT allelic form) reporter assays as previously described.14,17 The 293T reporter cells stably expressing different STING protein haplotypes (WT, HAQ, REF, AQ, or Q) were seeded at a density of 250,000 cells per cm^2 onto 96-well white poly(D-lysine) coated plates in 100 μl of DMEM with high glucose supplemented with 10% heat-inactivated FBS. The medium was removed the next day. 3-fold serial dilutions of compounds were prepared in digitonin buffer containing 50 mM HEPES (pH 7.0), 100 mM KCl, 3 mM MgCl$_2$, 0.1 mM DTT, 85 mM sucrose, 0.2% (w/w) BSA, 1 mM ATP, 0.1 mM GTP, and 10 μg/mL digitonin A. These diluted compounds were then added to the cells. After a 30-minute incubation at 37°C with 5% CO$_2$, the digitonin buffer was removed, and the cells were washed once with 100 μl of cultivation medium. Subsequently, 100 μl of fresh medium was added to each well. The plates with cells were further incubated for 5 hours at 37°C with 5% CO$_2$. After this incubation period, 50 μl of the medium was removed from each well, and 30 μl of the Bright-Glo Luciferase Assay System reagent (Promega) was added to each well. Luminescence was measured using a Spark instrument (TECAN, Grödig, Austria), and GraphPad Prism (La Jolla, USA) was used to calculate the 50% effective concentration (EC$_{50}$) from an 8-point dose–response curve. Representative dose–response curves can be found in Figure S1. Nonlinear regression curve fitting with standard slope was employed for EC$_{50}$ value calculations. The EC$_{50}$ value represents the concentration of cyclic dinucleotide (CDN) required to achieve half-maximal response of firefly luciferase in the 293T reporter assay.

Standard 293T STING reporter assay
The 293T reporter cells stably expressing WT STING protein haplotype were seeded into poly(D-lysine)-coated 96 (white) plates. The next day, the cells were treated with serially diluted compounds in a cell culture medium. The cells were incubated for 30 min, washed, and incubated for a further 6.5h or incubated for a complete period of 7h. After the incubation time, cells were washed and incubated for an additional 6.5h, or the complete 7h, the luminescence was measured using Bright-Glo Luciferase Assay System reagent (Promega) and the EC$_{50}$ values were calculated as described above.

Poxin activity assay
The activity of poxin towards MD1202D or MD 1203 was assessed by mixing 400 nM poxin with aforementioned compounds (20μM) in a reaction buffer This buffer contained phosphate-buffered saline at pH 7.4, 1 mM MgCl2, and 1 mM DTT. 2′3′ cGAMP and 3′3′ cGAMP served as controls. After a 12-hour incubation at 37°C, the reaction mixtures were analysed using Ultra-High Performance Liquid Chromatography-Mass Spectrometry (UPLC-MS). The measurements were performed on Waters UPLC-MS system. Reaction mixtures of 2′,3′ cGAMP and 3′,3′ cGAMP with or without poxin were analyzed on HILIC columns, while measurements of MD1202D and MD1203 were performed on C18 column. For all analyses, 2 microliters of the sample solution were injected onto the column. Conditions for MD1202D and MD1203 measurement were following: C18 (column: Waters Acquity UPLC BEH C18 column, 1.7 mm, 2.1 × 100 mm; LC method: H2O/ACN, 0.1% formic acid as a modifier, gradient 0–100 %, run length 7 min, flow 0.5 ml/min). Measurement of the 2′,3′ cGAMP and 3′,3′ cGAMP mixtures was performed on HILIC columns under these conditions: HILIC

(column: SeQuant ZIC-pHILIC, 5 μm, polymeric, 50 x 2.1 mm; LC method: CH3CN /0.01M aqueous ammonium acetate gradient 10–60 %, run length 7 min, flow 0.3 ml/min). Detection of the reaction mixtures was achieved by the UPLC photodiode array (PDA) detector which was followed in tandem with mass-spectrometry detector (QDa). The method used for mass detection was electro-spray ionization in positive (ESI+) or negative (ESI-) mode (cone voltage = 15 V, mass detector range 200–1000 Da).

QUANTIFICATION AND STATISTICAL ANALYSIS

Activity of CDNs in cell-based reporter assays

50% effective concentrations (EC_{50}) of CDNs represent the concentrations of CDNs required to achieve half-maximal response of firefly luciferase in the 293T reporter assay. The EC_{50} values were calculated from 8-point dose–response curves using nonlinear regression curve fitting with standard slope by GraphPad Prism software (La Jolla, USA). Representative dose–response curves are presented in Figure S1. Calculated EC_{50} values are presented in Table S1 and plotted in Figure 2. The EC_{50} values are expressed as mean values ± standard error of the mean (SEM) of two independent experiments (n=2) measured in triplicates.

Crystallographic data collection and processing

Statistics for crystallographic data collection and processing, structure solution and refinement were calculated with the phenix.table_one tool from the Phenix package v1.20.1-4487.[36] These statistics are summarized in Table S2.

Supplemental Information

Fluorinated cGAMP analogs, which act

as STING agonists and are not cleavable

by poxins: Structural basis of their function

Martin Klima, Milan Dejmek, Vojtech Duchoslav, Andrea Eisenreichova, Michal Sala, Karel Chalupsky, Dominika Chalupska, Barbora Novotná, Gabriel Birkuš, Radim Nencka, and Evzen Boura

Fluorinated cGAMP analogs, which act as STING agonists and are not cleavable by poxins: structural basis of their function
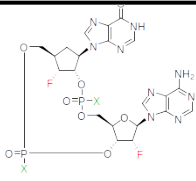
Martin Klima[1,#], Milan Dejmek[1,#], Vojtech Duchoslav[1,#], Andrea Eisenreichova[1], Michal Sala[1], Karel Chalupsky[1], Dominika Chalupska[1], Barbora Novotná[1], Gabriel Birkuš[1], Radim Nencka[1,*], Evzen Boura[1,2,*]

[1]Institute of Organic Chemistry and Biochemistry AS CR, v.v.i., Flemingovo nam. 2., 166 10 Prague 6, Czech Republic

[2]Lead contact

[#]These authors contributed equally.

*correspondence to nencka@uochb.cas.cz or boura@uochb.cas.cz

	X	DSF ΔTm (°C)[a] (±SEM)			Digitonin reporter assay EC$_{50}$ (µM)[b] (±SEM)				Std reporter assay EC$_{50}$ (µM)[c] (±SEM)
	X	WT	AQ	WT	HAQ	REF	AQ	Q	WT
2′3′cGAMP	O	15.3 ±0.17	22.7 ±0.19	0.02 ±0.004	0.02 ±0.003	0.07 ±0.02	0.04 ±0.01	0.05 ±0.02	36.91 ±8.02
ADU-S100	S	9.3 ±0.18	17.1 ±0.20	0.08 ±0.01	0.26 ±0.05	1.6 ±0.3	0.23 ±0.03	1.01 ±0.19	3.32 ±0.43
2′3′-c-dGdAMP[d]	O	13.5 ±0.25	20.4 ±0.18	0.05 ±0.02	0.02 ±0.01	3.3 ±0.9	0.03 ±0.01	0.06 ±0.03	75.4 ±25
MD1202D	S	13.4 ±0.3	21.3 ±0.1	0.02 ±0.01	0.03 ±0.01	0.36 ±0.17	0.02 ±0.01	0.38 ±0.22	1.45 ±0.95
MD1203	O	8.2 ±0.5	16.8 ±0.1	0.03 ±0.02	0.06 ±0.03	2.45 ±0.81	0.06 ±0.02	0.85 ±0.55	nd

[a]The values of the melting temperature (ΔT$_{m}$) assessed by differential scanning fluorimetry (DSF) with WT and AQ STING haplotypes; ΔT$_{m}$ values are expressed as mean ± standard error of the mean (SEM) of at least two independent experiments. [b]Results from the digitonin assay using 293T reporter cells expressing different STING protein haplotypes; EC$_{50}$ values are expressed as mean ± SEM of at least two independent experiments measured in triplicates. [c]Results of standard assay in 293T reporter cells expressing WT STING haplotype. EC$_{50}$ values are the mean of two independent experiments measured in triplicate. [d]Data partially published in.[1]

Table S1. **Activity of CDNs in the differential scanning fluorimetry, digitonin, and standard HEK 293T STING cell-based reporter assays.** Related to Figure 2.

Crystal		poxin/MD1203	poxin/MD1202D	STING/MD1203	STING/MD1202D
PDB accession code		8ORV	8P44	8ORW	8P45
Data collection and processing					
Diffraction source		BESSY 14.1	BESSY 14.1	BESSY 14.1	BESSY 14.1
Detector		Dectris Pilatus 6M	Dectris Pilatus 6M	Dectris Pilatus 6M	Dectris Pilatus 6M
Wavelength (Å)		0.9184	0.9184	0.9184	0.9184
Space group		C 2 2 2_1	P 1 2_1 1	C 1 2 1	C 1 2 1
Cell dimensions	a, b, c (Å)	54.1 95.5 93.5	54.2 91.2 93.1	89.4 78.1 35.9	89.5 78.0 35.4
	α, β, γ (°)	90.0 90.0 90.0	90.0 90.0 90.0	90.0 97.4 90.0	90.0 97.6 90.0
Resolution range (Å)		33.40 – 1.65 (1.71 – 1.65)	46.86 - 1.93 (2.00 - 1.93)	31.68 - 2.95 (3.01 - 2.95)	35.11 - 3.23 (3.35 - 3.23)
No. of total reflections		378,583 (33,821)	463,983 (46,880)	32,099 (3,178)	47,406 (2,548)
No. of unique reflections		29,391 (2,841)	66,736 (6,613)	4,988 (494)	3,917 (370)
Completeness (%)		99.47 (97.76)	97.86 (97.66)	95.11 (93.23)	99.90 (100.00)
Multiplicity		12.9 (11.9)	7.0 (7.1)	6.4 (6.4)	12.1 (6.9)
Mean I/σ(I)		14.98 (0.92)	8.17 (1.00)	6.43 (0.77)	8.20 (1.22)
Wilson B factor (Å^2)		24.19	26.56	75.27	90.47
R-merge		0.1307 (2.704)	0.2053 (2.153)	0.3852 (2.025)	0.3004 (1.940)
R-meas		0.1361 (2.824)	0.2217 (2.321)	0.4183 (2.197)	0.3135 (2.096)
CC1/2 (%)		99.9 (50.8)	99.7 (50.2)	98.5 (45.5)	99.5 (49.6)
CC* (%)		100.0 (82.1)	99.9 (81.8)	99.6 (79.1)	99.9 (81.4)
Structure solution and refinement					
R-work (%)		18.61 (52.92)	22.23 (31.17)	21.79 (29.59)	20.69 (35.05)
R-free (%)		22.08 (58.08)	26.09 (36.51)	24.82 (41.06)	25.83 (37.18)
CC-work (%)		97.1 (70.5)	95.3 (75.0)	90.6 (60.3)	94.4 (62.0)
CC-free (%)		96.7 (65.2)	93.9 (73.7)	97.4 (54.9)	92.6 (69.8)
R.m.s. deviations	bonds (Å)	0.030	0.006	0.029	0.003
	angles (°)	1.05	0.66	0.52	0.53
Average B factor (Å^2)	overall	24.95	31.40	73.01	87.15
	protein	23.00	30.54	73.53	87.81
	ligand	39.36	45.43	56.53	65.64
	solvent	34.24	36.13	N/A	N/A
Rotamer outliers (%)		0.62	0.00	0.00	0.00
Clashscore		0.00	1.74	0.00	0.00
Ramachandran (%)	favored	97.91	98.69	99.41	98.84
	allowed	2.09	1.31	0.59	1.16
	outliers	0.00	0.00	0.00	0.00

Table S2. **Statistics for data collection and processing, structure solution and refinement of the crystal structures of mpox virus poxin and human STING in complexes with MD1203 or MD1202D**. Related to STAR Methods. Numbers in parentheses refer to the highest resolution shell. R.m.s., root-mean-square.
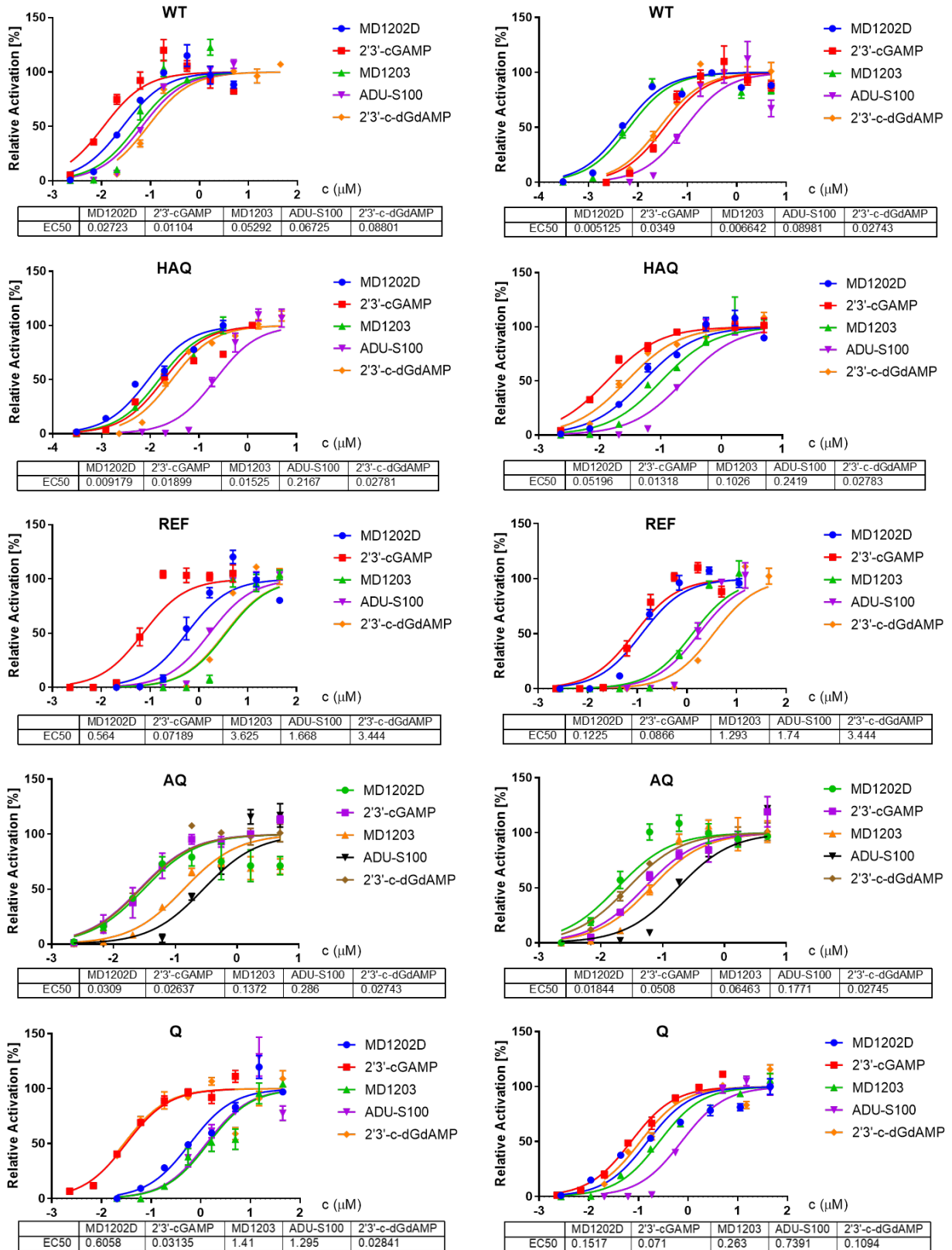
Figure S1. **Representative dose response curves from STING WT, HAQ, REF, AQ and Q from 293T reporter digitonin assays.** Related to Figure 2, data points are expressed as mean values ± standard deviations from measurements in triplicates.
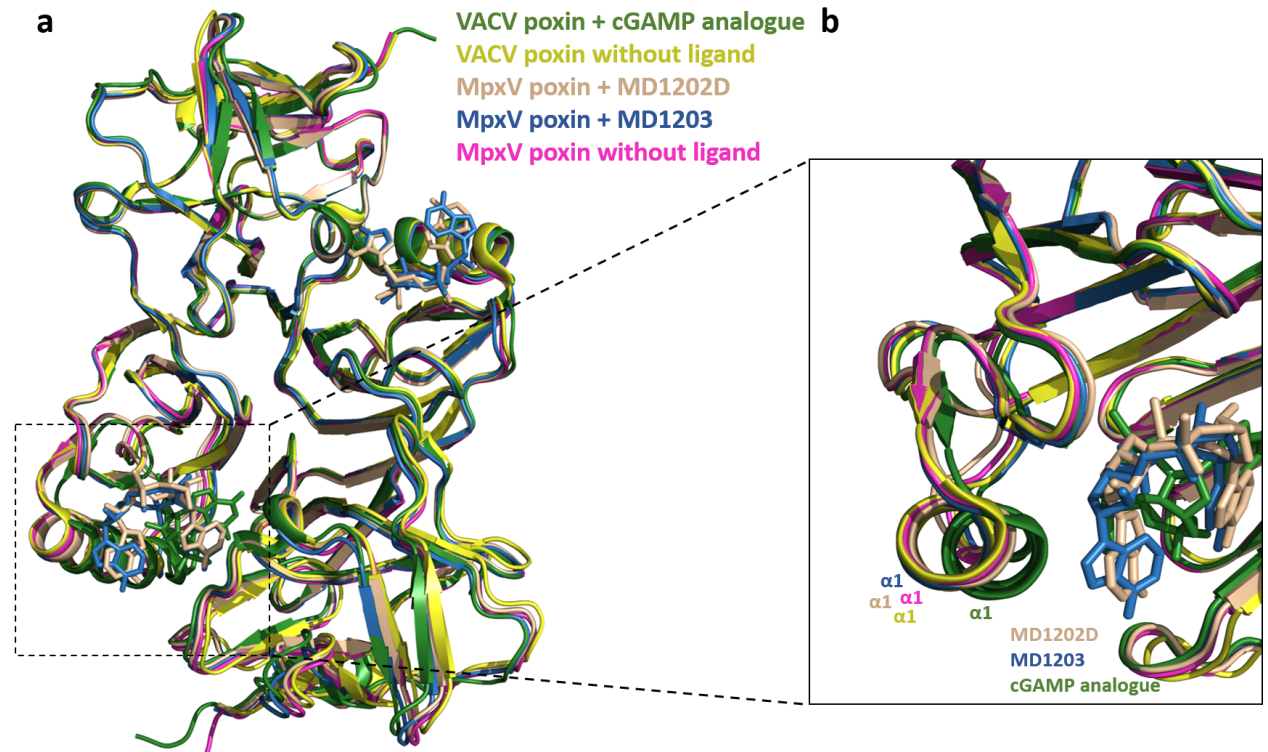
Figure S2. **Conformational changes induced in VACV poxin by ligand binding.** Related to Figure 6. **a)** Superposition of VACV poxin in a complex with an unhydrolyzable cGAMP analog depicted in green, VACV poxin without ligand depicted in yellow, MpxV poxin in complex with MD1202D depicted in light orange, MpxV poxin in complex with MD1203 depicted in blue and MpxV poxin without ligand depicted in pink. **b)** Close-up on the conformational changes of α-helix 1.

Supplementary References

1. Novotna, B., Vanekova, L., Zavrel, M., Budesinsky, M., Dejmek, M., Smola, M., Gutten, O., Tehrani, Z.A., Pimkova Polidarova, M., Brazdova, A., et al. (2019). Enzymatic Preparation of 2'-5',3'-5'-Cyclic Dinucleotides, Their Binding Properties to Stimulator of Interferon Genes Adaptor Protein, and Structure/Activity Correlations. J Med Chem *62*, 10676-10690. 10.1021/acs.jmedchem.9b01062.